

Search for Lepton Flavor Violating τ^- Decays into $\ell^- \eta$, $\ell^- \eta'$ and $\ell^- \pi^0$

Y. Miyazaki,²⁰ I. Adachi,⁷ H. Aihara,⁴³ D. Anipko,¹ K. Arinstein,¹ V. Aulchenko,¹
T. Aziz,³⁹ A. M. Bakich,³⁸ E. Barberio,¹⁹ A. Bay,¹⁶ I. Bedny,¹ K. Belous,⁹ U. Bitenc,¹²
I. Bizjak,¹² A. Bondar,¹ M. Bračko,^{7,18,12} T. E. Browder,⁶ A. Chen,²² W. T. Chen,²²
B. G. Cheon,³ Y. Choi,³⁷ Y. K. Choi,³⁷ J. Dalseno,¹⁹ S. Eidelman,¹ D. Epifanov,¹
S. Fratina,¹² N. Gabyshev,¹ A. Go,²² A. Gorišek,¹² H. Ha,¹⁴ J. Haba,⁷ K. Hayasaka,²⁰
H. Hayashii,²¹ M. Hazumi,⁷ D. Heffernan,³⁰ T. Hokuue,²⁰ Y. Hoshi,⁴¹ S. Hou,²²
W.-S. Hou,²⁴ T. Iijima,²⁰ A. Imoto,²¹ K. Inami,²⁰ A. Ishikawa,⁴³ R. Itoh,⁷ M. Iwasaki,⁴³
Y. Iwasaki,⁷ H. Kaji,²⁰ P. Kapusta,²⁵ H. Kawai,² T. Kawasaki,²⁷ H. Kichimi,⁷ Y. J. Kim,⁵
S. Korpar,^{18,12} P. Križan,^{17,12} P. Krokovny,⁷ R. Kulasiri,⁴ R. Kumar,³¹ C. C. Kuo,²²
A. Kuzmin,¹ Y.-J. Kwon,⁴⁸ M. J. Lee,³⁵ T. Lesiak,²⁵ S.-W. Lin,²⁴ F. Mandl,¹⁰
T. Matsumoto,⁴⁵ H. Miyake,³⁰ H. Miyata,²⁷ T. Nagamine,⁴² Y. Nagasaka,⁸ M. Nakao,⁷
S. Nishida,⁷ O. Nitoh,⁴⁶ S. Ogawa,⁴⁰ T. Ohshima,²⁰ S. Okuno,¹³ Y. Onuki,³³ H. Ozaki,⁷
P. Pakhlov,¹¹ G. Pakhlova,¹¹ H. Park,¹⁵ L. S. Peak,³⁸ R. Pestotnik,¹² L. E. Piilonen,⁴⁷
A. Poluektov,¹ H. Sahoo,⁶ Y. Sakai,⁷ N. Satoyama,³⁶ T. Schietinger,¹⁶ O. Schneider,¹⁶
J. Schümann,⁷ C. Schwanda,¹⁰ A. J. Schwartz,⁴ K. Senyo,²⁰ M. E. Seviour,¹⁹ H. Shibuya,⁴⁰
B. Shwartz,¹ V. Sidorov,¹ J. B. Singh,³¹ A. Somov,⁴ N. Soni,³¹ S. Stanič,²⁸ M. Starič,¹²
H. Stoeck,³⁸ T. Sumiyoshi,⁴⁵ F. Takasaki,⁷ K. Tamai,⁷ M. Tanaka,⁷ G. N. Taylor,¹⁹
Y. Teramoto,²⁹ X. C. Tian,³² I. Tikhomirov,¹¹ T. Tsukamoto,⁷ S. Uehara,⁷ K. Ueno,²⁴
Y. Unno,³ S. Uno,⁷ P. Urquijo,¹⁹ Y. Usov,¹ G. Varner,⁶ S. Villa,¹⁶ A. Vinokurova,¹
C. H. Wang,²³ M. Watanabe,²⁷ Y. Watanabe,⁴⁴ E. Won,¹⁴ A. Yamaguchi,⁴²
Y. Yamashita,²⁶ M. Yamauchi,⁷ Z. P. Zhang,³⁴ V. Zhilich,¹ V. Zhulanov,¹ and A. Zupanc¹²

(The Belle Collaboration)

¹*Budker Institute of Nuclear Physics, Novosibirsk, Russia*

²*Chiba University, Chiba, Japan*

³*Chonnam National University, Kwangju, South Korea*

⁴*University of Cincinnati, Cincinnati, OH, USA*

⁵*The Graduate University for Advanced Studies, Hayama, Japan*

⁶*University of Hawaii, Honolulu, HI, USA*

⁷*High Energy Accelerator Research Organization (KEK), Tsukuba, Japan*

⁸*Hiroshima Institute of Technology, Hiroshima, Japan*

⁹*Institute for High Energy Physics, Protvino, Russia*

¹⁰*Institute of High Energy Physics, Vienna, Austria*

¹¹*Institute for Theoretical and Experimental Physics, Moscow, Russia*

¹²*J. Stefan Institute, Ljubljana, Slovenia*

¹³*Kanagawa University, Yokohama, Japan*

¹⁴*Korea University, Seoul, South Korea*

- ¹⁵*Kyungpook National University, Taegu, South Korea*
- ¹⁶*Swiss Federal Institute of Technology of Lausanne, EPFL, Lausanne, Switzerland*
- ¹⁷*University of Ljubljana, Ljubljana, Slovenia*
- ¹⁸*University of Maribor, Maribor, Slovenia*
- ¹⁹*University of Melbourne, Victoria, Australia*
- ²⁰*Nagoya University, Nagoya, Japan*
- ²¹*Nara Women's University, Nara, Japan*
- ²²*National Central University, Chung-li, Taiwan*
- ²³*National United University, Miao Li, Taiwan*
- ²⁴*Department of Physics, National Taiwan University, Taipei, Taiwan*
- ²⁵*H. Niewodniczanski Institute of Nuclear Physics, Krakow, Poland*
- ²⁶*Nippon Dental University, Niigata, Japan*
- ²⁷*Niigata University, Niigata, Japan*
- ²⁸*University of Nova Gorica, Nova Gorica, Slovenia*
- ²⁹*Osaka City University, Osaka, Japan*
- ³⁰*Osaka University, Osaka, Japan*
- ³¹*Panjab University, Chandigarh, India*
- ³²*Peking University, Beijing, PR China*
- ³³*RIKEN BNL Research Center, Brookhaven, NY, USA*
- ³⁴*University of Science and Technology of China, Hefei, PR China*
- ³⁵*Seoul National University, Seoul, South Korea*
- ³⁶*Shinshu University, Nagano, Japan*
- ³⁷*Sungkyunkwan University, Suwon, South Korea*
- ³⁸*University of Sydney, Sydney, NSW, Australia*
- ³⁹*Tata Institute of Fundamental Research, Bombay, India*
- ⁴⁰*Toho University, Funabashi, Japan*
- ⁴¹*Tohoku Gakuin University, Tagajo, Japan*
- ⁴²*Tohoku University, Sendai, Japan*
- ⁴³*Department of Physics, University of Tokyo, Tokyo, Japan*
- ⁴⁴*Tokyo Institute of Technology, Tokyo, Japan*
- ⁴⁵*Tokyo Metropolitan University, Tokyo, Japan*
- ⁴⁶*Tokyo University of Agriculture and Technology, Tokyo, Japan*
- ⁴⁷*Virginia Polytechnic Institute and State University, Blacksburg, VA, USA*
- ⁴⁸*Yonsei University, Seoul, South Korea*

Abstract

We have searched for lepton-flavor-violating τ decays with a pseudoscalar meson (η , η' and π^0) using a data sample of 401 fb^{-1} collected with the Belle detector at the KEKB asymmetric-energy e^+e^- collider. No evidence for these decays is found and we set the following upper limits on the branching fractions: $\mathcal{B}(\tau^- \rightarrow e^- \eta) < 9.2 \times 10^{-8}$, $\mathcal{B}(\tau^- \rightarrow \mu^- \eta) < 6.5 \times 10^{-8}$, $\mathcal{B}(\tau^- \rightarrow e^- \eta') < 1.6 \times 10^{-7}$, $\mathcal{B}(\tau^- \rightarrow \mu^- \eta') < 1.3 \times 10^{-7}$, $\mathcal{B}(\tau^- \rightarrow e^- \pi^0) < 8.0 \times 10^{-8}$ and $\mathcal{B}(\tau^- \rightarrow \mu^- \pi^0) < 1.2 \times 10^{-7}$ at the 90% confidence level. These results improve our previously published upper limits by factors from 2.3 to 6.3.

PACS numbers: 11.30.Fs; 13.35.Dx; 14.60.Fg

INTRODUCTION

Lepton flavor violation (LFV) appears in various extensions of the Standard Model (SM), e.g., supersymmetry (SUSY), leptoquark and many other models. In particular, τ lepton-flavor-violating decays with a pseudoscalar meson ($M^0 = \eta, \eta'$ and π^0) are discussed in models with Higgs-mediated LFV processes [1, 2, 3], heavy singlet Dirac neutrinos [4], dimension-six effective fermionic operators that induce $\tau - \mu$ mixing [5], R -parity violation in SUSY [6, 7, 8], type III two-Higgs-doublet models [8] and flavor changing Z' bosons [8]. Some of these models predict branching fractions which, for certain combinations of model parameters, can be as high as 10^{-6} ; this rate is already accessible at high-statistics B factory experiments. Previously, we obtained 90% confidence level (C.L.) upper limits for various $\tau^- \rightarrow \ell^- M^0$ (where $\ell^- = e^-$ or μ^-) branching fractions using 154 fb^{-1} of data; the results were in the range $(1.5-10) \times 10^{-7}$ [9]. The BaBar collaboration has recently used 339 fb^{-1} of data to obtain 90% C.L. upper limits in the range $(1.1-2.4) \times 10^{-7}$ [10]. Here we update our previous results using 401 fb^{-1} of data. These datasets are collected at the $\Upsilon(4S)$ resonance and 60 MeV below it with the Belle detector at the KEKB e^+e^- asymmetric-energy collider [11].

The Belle detector is a large-solid-angle magnetic spectrometer that consists of a silicon vertex detector (SVD), a 50-layer central drift chamber (CDC), an array of aerogel threshold Cherenkov counters (ACC), a barrel-like arrangement of time-of-flight scintillation counters (TOF), and an electromagnetic calorimeter comprised of CsI(Tl) crystals (ECL), all located inside a superconducting solenoid coil that provides a 1.5 T magnetic field. An iron flux-return located outside the coil is instrumented to detect K_L^0 mesons and to identify muons (KLM). The detector is described in detail elsewhere [12].

Particle identification is very important for this measurement. We use particle identification likelihood variables based on the ratio of the energy deposited in the ECL to the momentum measured in the SVD and CDC, the shower shape in the ECL, the particle range in the KLM, the hit information from the ACC, the dE/dx information in the CDC, and the particle time-of-flight from the TOF. For lepton identification, we form likelihood ratios $\mathcal{P}(e)$ [13] and $\mathcal{P}(\mu)$ [14] based on the electron and muon probabilities, respectively, which are determined by the responses of the appropriate subdetectors.

In order to determine the event selection requirements, we use Monte Carlo (MC) samples. The following MC programs have been used to generate background events: KORALB/TAUOLA [15] for $\tau^+\tau^-$, QQ [16] for $B\bar{B}$ and continuum, BHLUMI [17] for Bhabha events, KKMC [18] for $e^+e^- \rightarrow \mu^+\mu^-$ and AAFH [19] for two-photon processes. Signal MC is generated by KORALB/TAUOLA. Signal τ decays are two-body and assumed to have a uniform angular distribution in the τ lepton's rest frame. All kinematic variables are calculated in the laboratory frame unless otherwise specified. In particular, variables calculated in the e^+e^- center-of-mass (CM) frame are indicated by the superscript "CM".

EVENT SELECTION

We search for $\tau^+\tau^-$ events in which one τ decays into a lepton and a pseudoscalar meson on the signal side, while the other τ decays into one charged track with a sign opposite to that of the signal-side lepton and any number of additional photons and neutrinos on the tag side. Thus, the decay chain we reconstruct is:

$$\{\tau^- \rightarrow \ell^- (e^- \text{ or } \mu^-) + M^0 (\eta, \eta' \text{ or } \pi^0)\} + \{\tau^+ \rightarrow (\text{a track})^+ + (n \geq 0 \gamma) + X(\text{missing})\}[\dagger].$$

We reconstruct a pseudoscalar meson in the following modes: $\eta \rightarrow \gamma\gamma$ and $\pi^+\pi^-\pi^0(\rightarrow \gamma\gamma)$, $\eta' \rightarrow \rho(\rightarrow \pi^+\pi^-)\gamma$ and $\eta(\rightarrow \gamma\gamma)\pi^+\pi^-$, and $\pi^0 \rightarrow \gamma\gamma$. While the $\pi^0 \rightarrow \gamma\gamma$ and $\eta \rightarrow \gamma\gamma$ modes correspond to a 1-1 prong configuration, the other modes give a 3-1 prong configuration. All charged tracks and photons are required to be reconstructed within the fiducial volume defined by $-0.866 < \cos\theta < 0.956$, where θ is the polar angle with respect to the direction along the e^+ beam. We select charged tracks with momenta transverse to the e^+ beam direction, $p_t > 0.1$ GeV/c while the photon energies must satisfy $E_\gamma > 0.1$ GeV (0.05 GeV) for the 1-1 prong (3-1 prong) configuration.

Candidate τ -pair events are thus required to have two and four tracks with a zero net charge for the 1-1 and 3-1 prong configurations, respectively. Event particles are separated into two hemispheres referred to as the signal and tag sides using the plane perpendicular to the thrust axis [20]. The tag side contains a single track, the signal side contains one or three tracks. The track on the signal side is required to be identified as a lepton. The electron (muon) identification criteria are $\mathcal{P}(e)$ ($\mathcal{P}(\mu)$) > 0.9 with $p > 0.7$ GeV/c. The efficiencies for electron and muon identification after these requirements are 92% and 88%, respectively. To reduce fake pseudoscalar meson candidates, we reject radiative photons from electrons on the signal side if $\cos\theta_{e\gamma} > 0.99$.

The π^0 candidates are formed from pairs of photons that satisfy $0.115 \text{ GeV}/c^2 < M_{\gamma\gamma} < 0.152 \text{ GeV}/c^2$, which corresponds to ± 2.5 standard deviations (σ) in terms of the mass resolution. We also require $p_{\pi^0} > 0.1$ GeV/c on the signal side.

The η meson is reconstructed in the $\gamma\gamma$ ($\pi^+\pi^-\pi^0$) decay modes. The mass window is chosen to be $0.515 \text{ GeV}/c^2$ ($0.532 \text{ GeV}/c^2$) $< m_{\gamma\gamma}(m_{\pi^+\pi^-\pi^0}) < 0.570 \text{ GeV}/c^2$ ($0.562 \text{ GeV}/c^2$), which corresponds to -3.0σ and $+2.5\sigma$ ($\pm 3\sigma$). To reduce background in $\eta \rightarrow \gamma\gamma$ channel, we reject those photons that form π^0 candidates in association with any other photon with $E_\gamma > 0.05$ GeV, within the π^0 mass window, $0.10 \text{ GeV}/c^2 < M_{\gamma\gamma} < 0.16 \text{ GeV}/c^2$.

The η' meson is reconstructed in the $\rho\gamma$ and $\eta\pi^+\pi^-$ decay modes. For the $\rho \rightarrow \pi^+\pi^-$ selection, the mass window is chosen to be $0.550 \text{ GeV}/c^2 < m_{\pi\pi} < 0.900 \text{ GeV}/c^2$. We reconstruct η' candidates using a ρ candidate and a photon on the signal side. The η' mass window is chosen to be $0.930 \text{ GeV}/c^2 < m_{\rho\gamma} < 0.970 \text{ GeV}/c^2$, which corresponds to -3.0σ and $+2.5\sigma$. Furthermore, we veto photons from π^0 candidates in order to avoid fake η' candidates from $\pi^0 \rightarrow \gamma\gamma$. We remove events if a π^0 candidate with invariant mass in the range $0.10 \text{ GeV}/c^2 < M_{\gamma\gamma} < 0.16 \text{ GeV}/c^2$ is reconstructed using a photon from the η' candidate and another photon with $E_\gamma > 0.05$ GeV. Figure 1 shows the $\rho \rightarrow \pi^+\pi^-$ and $\eta' \rightarrow \rho\gamma$ mass distributions. The dominant backgrounds for this mode come from $\tau^- \rightarrow h^- \rho^0 \nu_\tau (+\pi^0)$ (where $h^- = K^-$ or π^-) with a photon from π^0 decay, beam background or initial state radiation (ISR). As shown in Fig. 1, there is no η' peak either in data or in MC since decay modes with an η' are very rare and are not included in the generic τ decay model [21]. We also reconstruct η' candidates using an η candidate and two oppositely charged tracks consistent with being pions. We impose a $\gamma \rightarrow e^+e^-$ conversion veto as $P(e) < 0.1$ for both tracks in the η' candidate. The η products from $\eta' \rightarrow \eta\pi^+\pi^-$ decay are reconstructed using two photons. The η' mass window is chosen to be $0.920 \text{ GeV}/c^2 < m_{\eta\pi^+\pi^-} < 0.980 \text{ GeV}/c^2$, which corresponds to $\pm 3.0\sigma$.

[†] Unless otherwise stated, charge conjugate decays are implied throughout this paper.

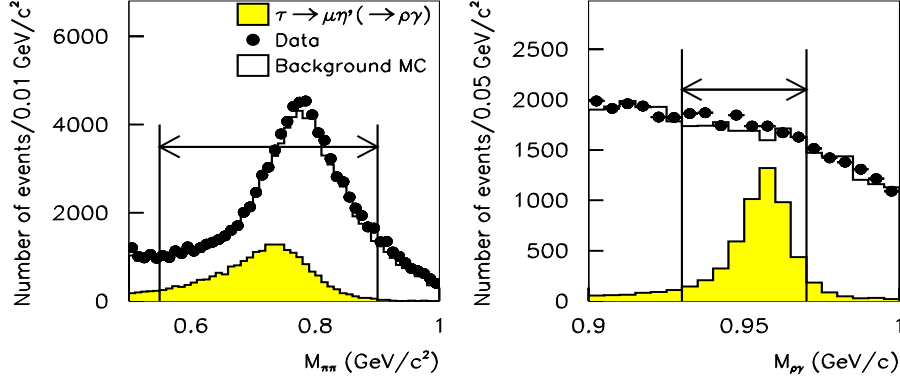


FIG. 1: The $\rho \rightarrow \pi^+\pi^-$ (left) and $\eta' \rightarrow \rho\gamma$ (right) mass distributions. While the signal MC ($\tau^- \rightarrow \mu^-\eta'$) distribution is normalized arbitrarily, the data and background MC are normalized to the same luminosity. Selected regions are indicated by the arrows from the marked cut boundaries.

To ensure that the missing particles are neutrinos rather than photons or charged particles that fall outside the detector acceptance, we impose additional requirements on the missing momentum vector \vec{p}_{miss} , which is calculated by subtracting the vector sum of the momenta of all tracks and photons from the sum of the e^+ and e^- beam momenta. We require that the magnitude of \vec{p}_{miss} be greater than $0.4 \text{ GeV}/c$, and that its direction point into the fiducial volume of the detector. Since neutrinos are normally emitted only on the tag side, the direction of \vec{p}_{miss} should lie within the tag side of the event. The cosine of the opening angle between \vec{p}_{miss} and the thrust axis (on the signal side) in the CM system, $\cos \theta_{\text{miss-thrust}}^{\text{CM}}$, is therefore required to be less than -0.55 .

For the 1-1 prong configuration, to suppress fake η (π^0) candidates arising from beam background and ISR, we require that the higher and lower energy photons ($E_{\gamma 1}$ and $E_{\gamma 2}$) in an η (π^0) candidate satisfy the requirement $E_{\gamma 1} > 0.6$ (0.9) GeV and $E_{\gamma 2} > 0.25$ (0.2) GeV , respectively, as shown for the $\tau^- \rightarrow \mu^-\pi^0$ mode in Figs. 2 (a) and (b). In order to suppress background from $q\bar{q}$ ($q = u, d, s, c$) continuum events, we require that the number of extra photon candidates on the signal and tag side (n_{γ}^{SIG} and n_{γ}^{TAG}) be $n_{\gamma}^{\text{SIG}} \leq 1$ and $n_{\gamma}^{\text{TAG}} \leq 2$, respectively. To reduce background from Bhabha and $\mu^+\mu^-$ events, we require the momentum of the lepton and that of the tag-side charged particle in the CM system to be less than $4.5 \text{ GeV}/c$. Furthermore, we require the momentum of a lepton to be greater than $1.5 \text{ GeV}/c$ for the $\tau^- \rightarrow \ell^-\pi^0$ mode (listed in Fig. 2 (c)). This condition is not imposed for the $\tau^- \rightarrow \ell^-\eta$ mode, in which the average lepton momentum as well as the background level are lower.

The reconstructed mass on the tag side using a track (with a pion mass hypothesis) and photons, m_{tag} , is required to be less than $1.777 \text{ GeV}/c^2$. The total visible energy in the CM frame, $E_{\text{vis}}^{\text{CM}}$, is defined as the sum of the energies of the η candidate, the lepton, the tag-side track (with a pion mass hypothesis) and all photon candidates. We require $E_{\text{vis}}^{\text{CM}}$ to satisfy the condition shown in Table I. To reduce background from $\mu^+\mu^-$, two-photon and Bhabha events, we add the veto condition $E_{\text{vis}}^{\text{CM}} > 8.5 \text{ GeV}$ for the muon (electron) mode if the track on the tag side is a muon (electron). The cosine of the opening angle between the lepton and the M^0 in the CM system, $\cos \theta_{\ell-M^0}^{\text{CM}}$, is required to lie in the range shown in Table I

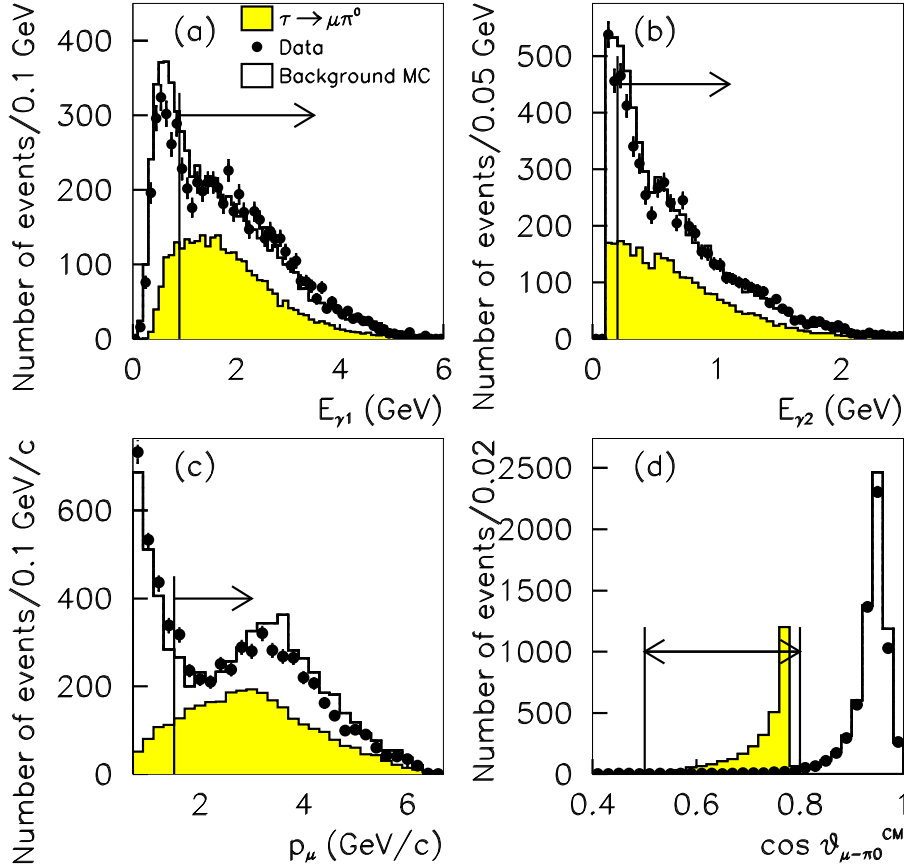


FIG. 2: Kinematic distributions used in the event selection: (a) higher energy and (b) lower energy of a photon from the π^0 candidate ($E_{\gamma 1}$ and $E_{\gamma 2}$); (c) momentum of a muon (p_{μ}); (d) the cosine of the opening angle between the muon and π^0 in the CM frame ($\cos \theta_{\mu-\pi^0}^{\text{CM}}$). While the signal MC ($\tau^- \rightarrow \mu^- \pi^0$) distribution is normalized arbitrarily, the data and background MC are normalized to the same luminosity. Selected regions are indicated by the arrows from the marked cut boundaries.

(also shown in Fig. 2 (d) for the $\tau^- \rightarrow \mu^- \pi^0$ mode). For all kinematic distributions in Fig. 2, reasonable agreement between the data and background MC is observed.

The correlation between the momentum of the track on the tag side, $p_{\text{tag}}^{\text{CM}}$, and the cosine of the opening angle between the thrust and missing particle, $\cos \theta_{\text{miss-thrust}}^{\text{CM}}$ in the CM system is employed to further suppress backgrounds from generic $\tau^+ \tau^-$ and $\mu^+ \mu^-$ events via the following requirements: $p_{\text{tag}}^{\text{CM}} > 1.1 \log(\cos \theta_{\text{miss-thrust}}^{\text{CM}} + 0.92) + 5.5$, and $p_{\text{tag}}^{\text{CM}} < 5 \cos \theta_{\text{miss-thrust}}^{\text{CM}} + 7.8$ where $p_{\text{tag}}^{\text{CM}}$ is in GeV/c (see Fig. 3). Finally, we require the following relation between the missing momentum p_{miss} and missing mass squared m_{miss}^2 to further suppress background from generic $\tau^+ \tau^-$ and continuum background. In signal events, two neutrinos are included if the τ decay on the tag side is a leptonic decay, while one neutrino is included if the τ decay on the tag side is a hadronic decay. Therefore, we separate events into two classes according to the track on the tag side: leptonic or hadronic, and apply the requirements

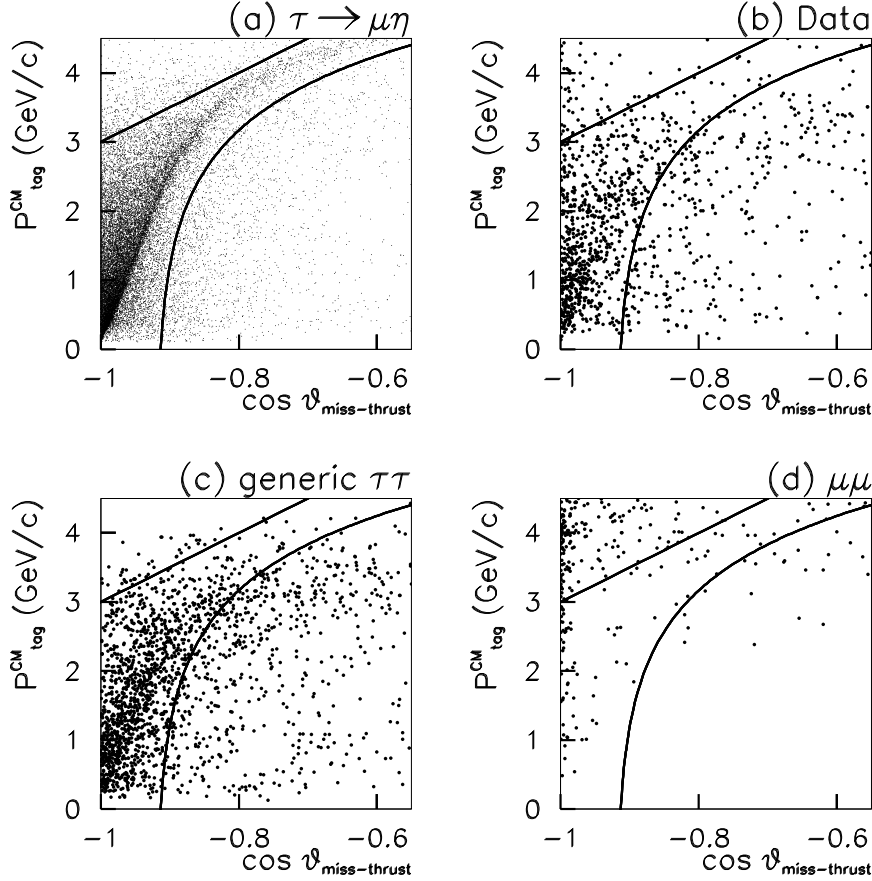


FIG. 3: Scatter-plots for (a) signal MC ($\tau^- \rightarrow \mu^- \eta (\rightarrow \gamma\gamma)$), (b) data, (c) generic $\tau^+ \tau^-$ MC events and (d) $\mu^+ \mu^-$ MC events in the $p_{\text{tag}}^{\text{CM}} - \cos \theta_{\text{miss-thrust}}$ plane. Selected regions lie between the two curves.

	$E_{\text{vis}}^{\text{CM}}$	$\cos \theta_{\ell-M^0}^{\text{CM}}$
$\tau^- \rightarrow \ell^- \eta$	$0.529 \text{ GeV} < E_{\text{vis}}^{\text{CM}} < 10.0 \text{ GeV}$	$0.50 < \cos \theta_{\ell-\eta}^{\text{CM}} < 0.85$
$\tau^- \rightarrow \ell^- \eta'$	$0.529 \text{ GeV} < E_{\text{vis}}^{\text{CM}} < 11.0 \text{ GeV}$	$0.50 < \cos \theta_{\ell-\eta'}^{\text{CM}}$
$\tau^- \rightarrow \ell^- \pi^0$	$0.529 \text{ GeV} < E_{\text{vis}}^{\text{CM}} < 10.0 \text{ GeV}$	$0.50 < \cos \theta_{\ell-\pi^0}^{\text{CM}} < 0.80$

TABLE I: The selection criteria for the total visible energy in the CM frame ($E_{\text{vis}}^{\text{CM}}$) and the cosine of the opening angle between the lepton and the M^0 in the CM system ($\cos \theta_{\ell-M^0}^{\text{CM}}$).

shown in Table II (see also Fig. 4).

For the 3-1 prong configuration, we impose similar requirements $m_{\text{tag}} < 1.777 \text{ GeV}/c^2$, $n_{\gamma}^{\text{SIG}} \leq 1$, $E_{\text{vis}}^{\text{CM}}$ and $\cos \theta_{\ell-M^0}^{\text{CM}}$ (Table I). For the $\eta' \rightarrow \rho\gamma$ mode, we require the photon energy to be greater than 0.25 GeV for the barrel and 0.40 GeV for the forward region to suppress fake candidates from beam background and ISR. The cut on the n_{γ}^{TAG} and $p_{\text{tag}}^{\text{CM}} - \cos \theta_{\text{miss-thrust}}^{\text{CM}}$ correlation is not applied for the 3-1 configuration modes, in which the background level is lower than in the 1-1 configuration modes. We apply requirements on p_{miss} and m_{miss}^2 similar

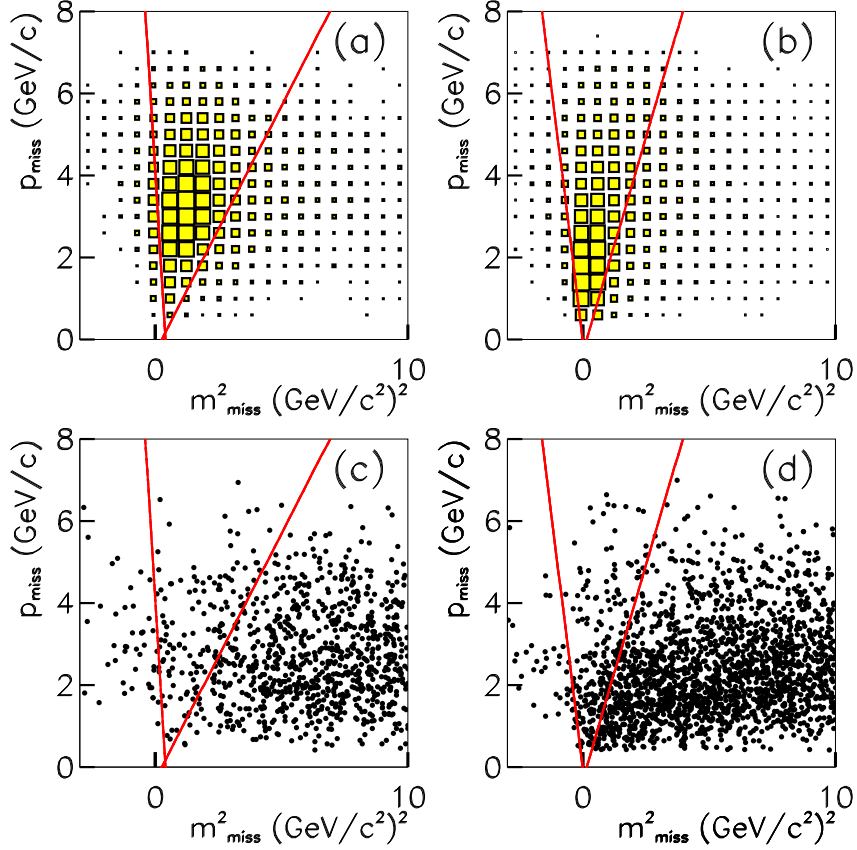


FIG. 4: Scatter-plots of $p_{\text{miss}} - m_{\text{miss}}^2$, for leptonic and hadronic tags: (a) shows the signal MC ($\tau^- \rightarrow \mu^- \eta$) distribution with arbitrary normalization for a leptonic tag while (c) shows the data distribution for a leptonic tag; (b) shows the signal MC ($\tau^- \rightarrow \mu^- \eta$) distribution with arbitrary normalization for a hadronic tag while Fig. (d) shows the data distribution for a hadronic tag. Selected regions are indicated by lines.

to those for the 1-1 prong configuration (see Table II).

SIGNAL REGION AND BACKGROUND ESTIMATION

Signal candidates are examined in the two-dimensional plots of the $\ell^- M^0$ invariant mass, M_{inv} , and the difference of their energy from the beam energy in the CM system, ΔE . A signal event should have M_{inv} close to the τ -lepton mass and ΔE close to zero. For all modes, the M_{inv} and ΔE resolutions are parameterized from the MC distributions with asymmetric Gaussian shapes to account for initial state radiation and ECL energy leakage for photons. The resolutions in M_{inv} and ΔE are given in Table III.

To evaluate the branching fractions, we use elliptical signal regions, which contain 90% of the MC signal events satisfying all cuts. These signal regions are shown in Fig. 5 and 6;

	Leptonic mode	Hadronic mode
$\eta \rightarrow \gamma\gamma$	$p_{\text{miss}} > -10m_{\text{miss}}^2 + 4$	$p_{\text{miss}} > -5m_{\text{miss}}^2 - 0.25$
	$p_{\text{miss}} > 1.1m_{\text{miss}}^2 - 0.3$	$p_{\text{miss}} > 2.1m_{\text{miss}}^2 - 0.3$
$\eta \rightarrow \pi^+\pi^-\pi^0$	$p_{\text{miss}} > -10m_{\text{miss}}^2 - 4$	$p_{\text{miss}} > -5m_{\text{miss}}^2 - 0.25$
	$p_{\text{miss}} > 1.1m_{\text{miss}}^2 - 1$	$p_{\text{miss}} > 2.1m_{\text{miss}}^2 - 0.3$
$\eta' \rightarrow \rho\gamma$	$p_{\text{miss}} > -8m_{\text{miss}}^2 - 0.2$	$p_{\text{miss}} > -5m_{\text{miss}}^2 - 0.2$
	$p_{\text{miss}} > 1.2m_{\text{miss}}^2 - 0.3$	$p_{\text{miss}} > 2m_{\text{miss}}^2 - 0.3$
$\eta' \rightarrow \eta\pi^+\pi^-$	$p_{\text{miss}} > -3m_{\text{miss}}^2$	$p_{\text{miss}} > -4m_{\text{miss}}^2 - 0.8$
	$p_{\text{miss}} > 1.5m_{\text{miss}}^2 - 0.5$	$p_{\text{miss}} > 2.5m_{\text{miss}}^2 - 0.2$
$\pi^0 \rightarrow \gamma\gamma$	$p_{\text{miss}} > -10m_{\text{miss}}^2 + 4$	$p_{\text{miss}} > -5m_{\text{miss}}^2 - 0.25$
	$p_{\text{miss}} > 1.1m_{\text{miss}}^2 - 0.3$	$p_{\text{miss}} > 2.1m_{\text{miss}}^2 - 0.3$

TABLE II: The selection criteria for the missing momentum (p_{miss}) and missing mass squared (m_{miss}^2) correlations, p_{miss} is in GeV/c and m_{miss}^2 is in (GeV/c²)².

Mode	$\sigma_{M_{\text{inv}}}^{\text{high}}$ (MeV/c ²)	$\sigma_{M_{\text{inv}}}^{\text{low}}$ (MeV/c ²)	$\sigma_{\Delta E}^{\text{high}}$ (MeV)	$\sigma_{\Delta E}^{\text{low}}$ (MeV)
$\mu\eta(\rightarrow \gamma\gamma)$	14.7	19.4	30.3	61.4
$\mu\eta(\rightarrow \pi^+\pi^-\pi^0)$	7.2	8.5	18.5	36.4
$e\eta(\rightarrow \gamma\gamma)$	14.0	19.8	37.3	62.4
$e\eta(\rightarrow \pi^+\pi^-\pi^0)$	7.6	9.3	19.4	41.8
$\mu\eta'(\rightarrow \rho\gamma)$	7.8	9.0	16.8	34.1
$\mu\eta'(\rightarrow \eta\pi^+\pi^-)$	11.2	19.1	27.1	53.5
$e\eta'(\rightarrow \rho\gamma)$	9.2	10.4	19.6	40.0
$e\eta'(\rightarrow \eta\pi^+\pi^-)$	10.3	21.9	26.1	59.4
$\mu\pi^0(\rightarrow \gamma\gamma)$	14.9	19.1	33.8	63.0
$e\pi^0(\rightarrow \gamma\gamma)$	12.7	23.1	35.6	64.6

TABLE III: Summary of M_{inv} (MeV/c²) and ΔE resolutions (MeV)

the corresponding signal efficiencies are given in Table IV. We blind the signal region so as not to bias our choice of selection criteria. Figures 5 and 6 show scatter-plots for data and signal MC samples distributed over $\pm 10\sigma$ in the $M_{\text{inv}} - \Delta E$ plane. Most of the surviving background events in $\tau \rightarrow \ell\pi^0$ modes come from $\tau^- \rightarrow \pi^-\pi^0\nu_\tau$, where the π^- is misidentified as a lepton. The remaining backgrounds in the $\tau^- \rightarrow \mu^-\eta(\rightarrow \gamma\gamma)$ mode are from τ decay including a real η meson or combinations of a fake lepton and a fake η meson formed by γ 's from π^0 decay, ISR or beam background. As there are few remaining MC background events in the signal ellipse, we estimate the background contribution using the M_{inv} sideband regions. Extrapolation to the signal region assumes that the background distribution is flat along the M_{inv} axis. We then estimate the expected number of the background events in the signal region for each mode using the number of data events observed in the sideband region inside the horizontal lines but excluding the signal region as shown in Fig. 5 and 6. The numbers of background events in the 90% elliptical signal region are also shown in Table IV.

Mode	\mathcal{B}_{M^0}	ε (%)	b_0	s	Total Sys. (%)	s_{90}
$\tau \rightarrow \mu\eta(\rightarrow \gamma\gamma)$	0.3938	6.42	0.40 ± 0.29	0	7.1	2.1
$\tau \rightarrow \mu\eta(\rightarrow \pi^+\pi^-\pi^0)$	0.227	6.84	0.24 ± 0.24	0	5.6	2.2
$\tau \rightarrow e\eta(\rightarrow \gamma\gamma)$	0.3938	4.57	0.25 ± 0.25	0	7.1	2.2
$\tau \rightarrow e\eta(\rightarrow \pi^+\pi^-\pi^0)$	0.227	4.72	0.53 ± 0.53	0	5.6	2.0
$\tau \rightarrow \mu\eta'(\rightarrow \rho\gamma)$	0.294×1.0	5.40	0.23 ± 0.23	0	6.8	2.2
$\tau \rightarrow \mu\eta'(\rightarrow \eta\pi^+\pi^-)$	0.445×0.3943	4.92	$0.0_{-0.0}^{+0.23}$	0	8.3	2.5
$\tau \rightarrow e\eta'(\rightarrow \rho\gamma)$	0.294×1.0	4.76	$0.0_{-0.0}^{+0.33}$	0	6.8	2.5
$\tau \rightarrow e\eta'(\rightarrow \eta\pi^+\pi^-)$	0.445×0.3943	4.27	$0.0_{-0.0}^{+0.24}$	0	8.3	2.5
$\tau \rightarrow \mu\pi^0(\rightarrow \gamma\gamma)$	0.98798	4.53	0.58 ± 0.34	1	4.5	3.8
$\tau \rightarrow e\pi^0(\rightarrow \gamma\gamma)$	0.98798	3.93	0.20 ± 0.20	0	4.5	2.2

TABLE IV: Results of the final event selection for the individual modes: \mathcal{B}_{M^0} is the branching fraction for the M^0 decay; b_0 and s are the number of expected background and observed events in the signal region, respectively; “Total sys.” means the total systematic uncertainty; s_{90} is the upper limit on the number of signal events including systematic uncertainties.

Systematic uncertainties for M^0 reconstruction are estimated to be 3.0%, 4.0%, 4.0%, 5.0% and 3.0% for $\eta \rightarrow \gamma\gamma$, $\eta \rightarrow \pi^+\pi^-\pi^0$, $\eta' \rightarrow \rho\gamma$, $\eta' \rightarrow \eta\pi^+\pi^-$ and $\pi^0 \rightarrow \gamma\gamma$, respectively. Furthermore, the uncertainties due to the branching fractions of the M^0 meson are 0.7%, 1.8%, 3.1% and 3.1% for $\eta \rightarrow \gamma\gamma$, $\eta \rightarrow \pi^+\pi^-\pi^0$, $\eta' \rightarrow \rho\gamma$ and $\eta' \rightarrow \eta\pi^+\pi^-$, respectively [21]. For the π^0 veto we assign a 5.5% uncertainty for the $\eta \rightarrow \gamma\gamma$ mode while a 2.8% uncertainty is assigned to the $\eta' \rightarrow \rho\gamma$ mode. The uncertainties in the trigger (0.5–1.0%), tracking for lepton on the signal side and track on the tag side (1.0% per each track), lepton identification (2.0%), MC statistics (1.0–1.5%) and luminosity (1.4%) are also considered. All these uncertainties are added in quadrature, and the total systematic uncertainties are shown in Table IV.

While the angular distribution of signal τ decays is initially assumed to be uniform in this analysis, it is sensitive to the lepton-flavor-violating interaction structure [22]. The spin correlation between the τ lepton on the signal and that on the tag side must be considered. A possible nonuniformity is taken into account by comparing the uniform case with MC’s assuming $V - A$ and $V + A$ interactions, which result in the maximum possible variations. No statistically significant difference in the $M_{\text{inv}} - \Delta E$ distribution or the efficiencies is found compared to the case of the uniform distribution. Therefore, systematic uncertainties due to these effects are neglected in the upper limit evaluation.

We open the blind and find only one event in $\tau \rightarrow \mu\pi^0(\rightarrow \gamma\gamma)$. In other modes, no events are found in the blinded region. Since no statistically significant excess of data over the expected background in the signal region is observed, we set upper limits for branching fractions. The upper limit on the number of signal events at the 90% C.L. s_{90} including systematic uncertainty is obtained with the use of the Feldman-Cousins method [23] calculated by the POLE program without conditioning [24]. The upper limit on the branching fraction (\mathcal{B}) is then given by

$$\mathcal{B}(\tau^- \rightarrow \ell^- M^0) < \frac{s_{90}}{2N_{\tau\tau\varepsilon\mathcal{B}_{M^0}}}, \quad (1)$$

Mode	M^0 subdecay mode	Upper limit on \mathcal{B} at 90% C.L.
$\tau^- \rightarrow \mu^- \eta$	$\eta \rightarrow \gamma\gamma$	1.2×10^{-7}
	$\eta \rightarrow \pi^+ \pi^- \pi^0$	2.0×10^{-7}
	Combined	6.5×10^{-8}
$\tau^- \rightarrow e^- \eta$	$\eta \rightarrow \gamma\gamma$	1.7×10^{-7}
	$\eta \rightarrow \pi^+ \pi^- \pi^0$	2.6×10^{-7}
	Combined	9.2×10^{-8}
$\tau^- \rightarrow \mu^- \eta'$	$\eta' \rightarrow \rho\gamma$	1.9×10^{-7}
	$\eta' \rightarrow \eta\pi^+\pi^-$	4.1×10^{-7}
	Combined	1.3×10^{-7}
$\tau^- \rightarrow e^- \eta'$	$\eta' \rightarrow \rho\gamma$	2.5×10^{-7}
	$\eta' \rightarrow \eta\pi^+\pi^-$	4.7×10^{-7}
	Combined	1.6×10^{-7}
$\tau^- \rightarrow \mu^- \pi^0$	$\pi^0 \rightarrow \gamma\gamma$	1.2×10^{-7}
$\tau^- \rightarrow e^- \pi^0$	$\pi^0 \rightarrow \gamma\gamma$	8.0×10^{-8}

TABLE V: Summary of upper limits on \mathcal{B} at 90% C.L.

where \mathcal{B}_{M^0} is taken from Ref. [21] and $N_{\tau\tau} = 357.7 \times 10^6$ is the number of $\tau^+\tau^-$ pairs produced in 401 fb^{-1} of data. We obtain $N_{\tau\tau}$ using $\sigma_{\tau\tau} = 0.892 \pm 0.002 \text{ nb}$, the $e^+e^- \rightarrow \tau^+\tau^-$ cross section at the $\Upsilon(4S)$ resonance calculated by KKMC [18]. The combined upper limits for the η and η' modes are obtained by summing $\epsilon\mathcal{B}$, the observed and expected background events of each subdecay, and systematic uncertainties are estimated by first summing all correlated terms linearly and then adding quadratically the uncorrelated terms. The upper limits for the branching fractions $\mathcal{B}(\tau^- \rightarrow \ell^- M^0)$ are in the range $(6.5 - 16) \times 10^{-8}$ at the 90% confidence level. A summary of the upper limits is given in Table V. These results improve our previously published upper limits [9] by factors of 2.3–6.3. They also improve upon the recent BaBar results [10] by factors of ~ 1.5 .

DISCUSSION

The branching fraction for the $\tau^- \rightarrow \mu^- \eta$ mode may be enhanced by Higgs-mediated LFV if large mixing between left-hand scalar muons and scalar taus in the corresponding SUSY model occurs [1]. This can be written as

$$\mathcal{B}(\tau^- \rightarrow \mu^- \eta) = 8.4 \times 10^{-7} \left(\frac{\tan \beta}{60} \right)^6 \left(\frac{100 \text{ GeV}/c^2}{m_A} \right)^4, \quad (2)$$

where m_A is the pseudoscalar Higgs mass and $\tan \beta$ is the ratio of the vacuum expectation values of the neutral Higgs fields coupled to up-type and down-type fermions. From our upper limit on the branching fraction for the decay $\tau^- \rightarrow \mu^- \eta$, some region of m_A and $\tan \beta$ parameters can be excluded. Figure 7 shows the excluded region in the $m_A - \tan \beta$ plane. It also shows the constraints at a 95% C.L. from the CDF [25], DØ [26] and LEP2 experiments [27]. The excluded regions from these experiments are shown with the Higgs

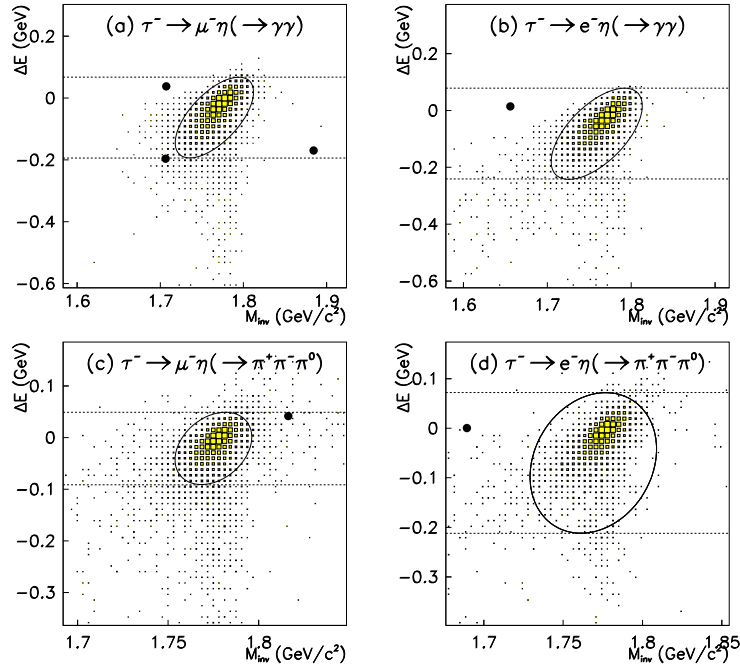


FIG. 5: Scatter-plots of data in the $M_{\text{inv}} - \Delta E$ plane: (a), (b), (c) and (d) correspond to the $\pm 10\sigma$ area for the $\tau^- \rightarrow \mu^- \eta (\rightarrow \gamma\gamma)$, $\tau^- \rightarrow e^- \eta (\rightarrow \gamma\gamma)$, $\tau^- \rightarrow \mu^- \eta (\rightarrow \pi^+ \pi^- \pi^0)$ and $\tau^- \rightarrow e^- \eta (\rightarrow \pi^+ \pi^- \pi^0)$ modes, respectively. The filled boxes show the MC signal distribution with arbitrary normalization. The elliptical signal region shown by the solid curve is used for evaluating the signal yield. The region between the horizontal lines excluding the signal region is used to estimate the expected background in the elliptical region.

mass parameter $\mu > 0$ in the maximum stop-mixing scenario [28]. We note that their theoretical assumptions are somewhat different with from ours, and thus these regions are for illustrative purposes only.

The improved sensitivity to rare τ lepton decay achieved in this work can also be used to constrain the parameters of other models, e.g., those with the heavy Dirac neutrinos [4]. In this model, the expected branching fractions of various LFV decays are evaluated in terms of combinations of the model parameters. These parameters, denoted $y_{\tau e}$ and $y_{\tau \mu}$ for τ decay involving an electron and a muon, respectively, can vary from 0 to 1. We obtain the following upper limits: $y_{\tau e} < 0.17$ and $y_{\tau \mu} < 0.47$ at 90% C.L. from our $\tau^- \rightarrow \ell^- \pi^0$ results.

SUMMARY

We have searched for lepton-flavor-violating τ decays with a pseudoscalar meson (η , η' and π^0) using 401 fb^{-1} of data. No signal is found and we set the following upper limits on branching fractions: $\mathcal{B}(\tau^- \rightarrow e^- \eta) < 9.2 \times 10^{-8}$, $\mathcal{B}(\tau^- \rightarrow \mu^- \eta) < 6.5 \times 10^{-8}$, $\mathcal{B}(\tau^- \rightarrow e^- \eta')$ $< 1.6 \times 10^{-7}$, $\mathcal{B}(\tau^- \rightarrow \mu^- \eta')$ $< 1.3 \times 10^{-7}$, $\mathcal{B}(\tau^- \rightarrow e^- \pi^0) < 8.0 \times 10^{-8}$ and $\mathcal{B}(\tau^- \rightarrow \mu^- \pi^0) < 1.2 \times 10^{-7}$ at the 90% confidence level, respectively. These results improve upon our previously published upper limits by factors from 2.3 to 6.3. They are also somewhat better than the recent results from BaBar [10] with the single exception of

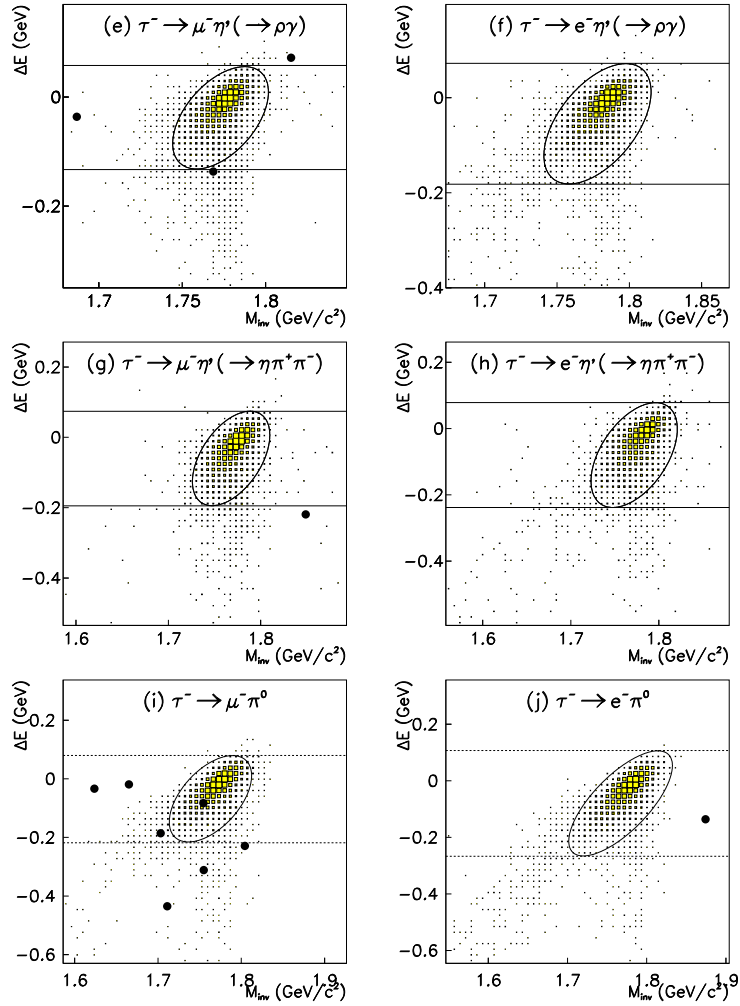


FIG. 6: Scatter-plots of data in the $M_{\text{inv}} - \Delta E$ plane: (e), (f), (g), (h), (i) and (j) correspond to the $\pm 10\sigma$ area for the $\tau^- \rightarrow \mu^- \eta' (\rightarrow \rho \gamma)$, $\tau^- \rightarrow e^- \eta' (\rightarrow \rho \gamma)$, $\tau^- \rightarrow \mu^- \eta' (\rightarrow \eta \pi^+ \pi^-)$, $\tau^- \rightarrow e^- \eta' (\rightarrow \eta \pi^+ \pi^-)$, $\tau^- \rightarrow \mu^- \pi^0 (\rightarrow \gamma \gamma)$ and $\tau^- \rightarrow e^- \pi^0 (\rightarrow \gamma \gamma)$ modes, respectively. The data are indicated by the solid circles. The filled boxes show the MC signal distribution with arbitrary normalization. The elliptical signal region shown by the solid curve is used for evaluating the signal yield. The region between the horizontal lines excluding the signal region is used to estimate the expected background in the elliptical region.

the limit for the $\tau^- \rightarrow \mu^- \pi^0$ mode, and are the most stringent limits on these modes to date. These limits help to constrain new physics scenarios beyond the Standard Model.

Acknowledgments

We are grateful to A. Brignole and A. Rossi for enlightening discussions. We thank the KEKB group for the excellent operation of the accelerator, the KEK cryogenics group for the efficient operation of the solenoid, and the KEK computer group and the National Institute

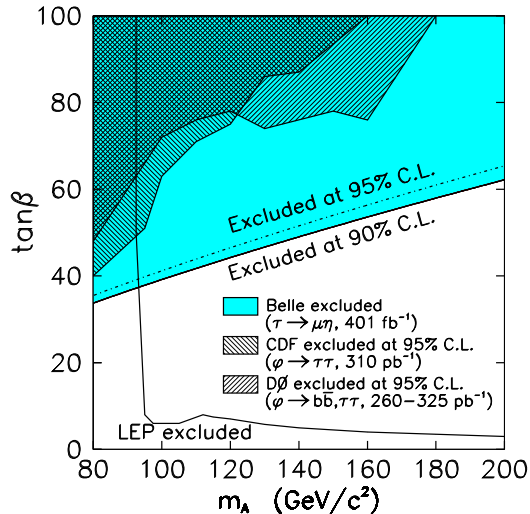


FIG. 7: The excluded region in the $m_A - \tan\beta$ plane from our results at 90% C.L. and other experiments at 95% C.L. from CDF [25], DØ [26], LEP [27]. The excluded regions from the CDF, DØ and LEP2 experiments are shown for $\mu > 0$ in the maximum stop-mixing scenario [28].

of Informatics for valuable computing and Super-SINET network support. We acknowledge support from the Ministry of Education, Culture, Sports, Science, and Technology of Japan and the Japan Society for the Promotion of Science; the Australian Research Council and the Australian Department of Education, Science and Training; the National Science Foundation of China and the Knowledge Innovation Program of the Chinese Academy of Sciences under contract No. 10575109 and IHEP-U-503; the Department of Science and Technology of India; the BK21 program of the Ministry of Education of Korea, the CHEP SRC program and Basic Research program (grant No. R01-2005-000-10089-0) of the Korea Science and Engineering Foundation, and the Pure Basic Research Group program of the Korea Research Foundation; the Polish State Committee for Scientific Research; the Ministry of Education and Science of the Russian Federation and the Russian Federal Agency for Atomic Energy; the Slovenian Research Agency; the Swiss National Science Foundation; the National Science Council and the Ministry of Education of Taiwan; and the U.S. Department of Energy.

-
- [1] M. Sher, Phys. Rev. D **66**, 057301 (2002).
 - [2] A. Brignole and A. Rossi, Nucl. Phys. B **701**, 3 (2004).
 - [3] C.-H. Chen and C.-Q. Geng, Phys. Rev. D **74**, 035010 (2006).
 - [4] A. Ilakovac, Phys. Rev. D **62**, 036010 (2000).
 - [5] D. Black *et al.*, Phys. Rev. D **66**, 053002 (2002).
 - [6] J. P. Saha and A. Kundu, Phys. Rev. D **66**, 054021 (2002).
 - [7] R. Barbier *et al.*, Phys. Rep. **420**, 1 (2005).
 - [8] W.-J. Li, Y.-D. Yang and X.-D. Zhang, Phys. Rev. D **73**, 073005 (2006).
 - [9] Y. Enari *et al.* (Belle Collaboration), Phys. Lett. B **622**, 218 (2005).
 - [10] B. Aubert *et al.* (BaBar Collaboration), Phys. Rev. Lett. **98**, 061803 (2007).

- [11] S. Kurokawa and E. Kikutani, Nucl. Instr. and Meth. A **499**, 1 (2003), and other papers included in this Volume.
- [12] A. Abashian *et al.* (Belle Collaboration), Nucl. Instr. and Meth. A **479**, 117 (2002).
- [13] K. Hanagaki *et al.*, Nucl. Instr. and Meth. A **485**, 490 (2002).
- [14] A. Abashian *et al.*, Nucl. Instr. and Meth. A **491**, 69 (2002).
- [15] S. Jadach and Z. Wąs, Comp. Phys. Commun. **85**, 453 (1995).
- [16] QQ is an event generator developed by the CLEO Collaboration and described in <http://www.lns.cornell.edu/public/CLEO/soft/qq/>. It is based on the LUND Monte Carlo for jet fragmentation and e^+e^- physics described in T. Sjöstrand, Comp. Phys. Commun. **39**, 347 (1986) and T. Sjöstrand, Comp. Phys. Commun. **43**, 367 (1987).
- [17] S. Jadach *et al.*, Comp. Phys. Commun. **79**, 305 (1992).
- [18] S. Jadach *et al.*, Comp. Phys. Commun. **130**, 260 (2000).
- [19] F. A. Berends *et al.*, Comp. Phys. Commun. **40**, 285 (1986).
- [20] S. Brandt *et al.*, Phys. Lett. **12**, 57 (1964); E. Farhi, Phys. Rev. Lett. **39**, 1587 (1977).
- [21] W.-M. Yao *et al.* (Particle Data Group), J. Phys. G **33**, 1 (2006).
- [22] R. Kitano and T. Okada, Phys. Rev. D **63**, 3873 (2001).
- [23] G. J. Feldman and R. D. Cousins, Phys. Rev. D **57**, 3873 (1998).
- [24] See <http://www3.tsl.uu.se/~conrad/pole.html>, J. Conrad *et al.*, Phys. Rev. D **67**, 012002 (2003).
- [25] A. Abulencia *et al.* (CDF Collaboration), Phys. Rev. Lett. **96**, 011802 (2006).
- [26] V. M. Abazov *et al.* (DØ Collaboration), Phys. Rev. Lett. **95**, 151801 (2005); V. M. Abazov *et al.* (DØ Collaboration), Phys. Rev. Lett. **97**, 121802 (2006).
- [27] The ALEPH, DELPHI, L3 and OPAL Collaboration, LEP Higgs Working Group, LHWG-Note 2005-01, http://lephiggs.web.cern.ch/LEPHIGGS/papers/July2005_MSSM/.
- [28] M. Carena, S. Heinemeyer, C. E. M. Wagner and G. Weiglein, Eur. Phys. J. C **95**, 601 (2003).